EUROPEAN TRANSACTIONS ON ELECTRICAL POWER
Euro. Trans. Electr. Power 2011; **21**:1159–1177
Published online 14 January 2010 in Wiley Online Library (wileyonlinelibrary.com). DOI: 10.1002/etep.407

Advanced control and management functionalities for multi-microgrids

A. G. Madureira[1]*,†, J. C. Pereira[1], N. J. Gil[1], J. A. Peças Lopes[1], G. N. Korres[2] and N. D. Hatziargyriou[2]

[1]*Institute for Systems and Computer Engineering of Porto and Faculty of Engineering of Porto University, Porto, Portugal*
[2]*Electrical and Computer Engineering, National Technical University of Athens, Athens, Greece*

SUMMARY

This paper addresses the extension of the microgrid concept, following a massive integration of these active cells in power distribution networks, by adopting a coordinated management strategy together with distributed generation units directly connected to the medium voltage distribution network. In order to achieve this, a technical and commercial management scheme must be developed for coordinated control of a distribution system with multi-microgrids, which should take into account the specific technical capabilities and characteristics of each type of generating source. In particular, tools for coordinated voltage support and frequency control, as well as for state estimation have been developed for this type of network. Concerning voltage support, a new methodology exploiting an optimization tool based on a meta-heuristic approach was developed. For state estimation, two approaches were considered: multi-microgrid state estimation and fuzzy state estimation. Regarding frequency control, the hierarchical structure of the multi-microgrid is exploited to deal with the transition to islanded operation and load following in islanded operation. All these tools have proved to be efficient in managing the multi-microgrid system in normal interconnected mode and, in case of the frequency control, in islanded operation. Copyright © 2010 John Wiley & Sons, Ltd.

KEY WORDS: microgrids; multi-microgrids; voltage control; frequency control; state estimation

1. INTRODUCTION

The need of reducing CO_2 emissions in the electricity generation field, recent technological developments particularly for distributed generation (DG) and electricity business restructuring have been some of the key factors responsible for the growing penetration of DG in power distribution grids. In addition to DG penetration, the connection of small generating units directly to the low voltage (LV) distribution network is expected to become a reality in a near future, thus creating autonomous active cells called microgrids.

A microgrid can be defined as an LV feeder with several microsources (such as microturbines, photovoltaic (PV) panels, etc.) together with storage devices and controllable loads connected on that same feeder and managed by a hierarchical control system [1]. These LV microgrids may be operated in interconnected or islanded mode (under emergency conditions). Therefore, the adoption of the microgrid concept will allow an improvement in the quality of service, lead to reduced green house gases (GHG) emissions through reduction of losses in the distribution grid and potentially reduction of electricity supply costs.

This work aims at studying the increase of microgeneration penetration in electrical networks through the exploitation and extension of the microgrid concept, involving the development of new tools for multi-microgrid management and operation (involving Distribution Management System (DMS) architecture and new software adaptation).

*Correspondence to: A. G. Madureira, INESC Porto, Power Systems Unit, FEUP, DEEC, Portugal.
†E-mail: agm@inescporto.pt

This work moves on to consider the new concept of multi-microgrids. This requires a higher-level structure, formed at the Medium Voltage (MV) level, consisting of LV microgrids and DG units connected on several adjacent MV feeders. Microgrids, DG units, and MV loads under demand side management (DSM) control can be considered in this network, for the purpose of control and management, as active cells. The development of this concept poses challenging problems due to the increase in network dimension and operation complexity, since a large number of LV microsources and loads need to operate together in a coordinated way.

In addition, it will be necessary to integrate these microgrids with existing DG units, directly connected into the MV network, as well as some large MV equivalent loads that may be under a DSM operation or load curtailment strategy for providing ancillary services. This involves the adaptation and development of new DMS tools to be able to deal with such a demanding operating scenario. An effective management of this type of system requires the development of a hierarchical control architecture, where intermediate control will be exercised by an intermediate controller to be installed at the MV bus level of an HV/MV substation, under the responsibility of the distribution system operator (DSO) and will be in charge of each multi-microgrid. In this way, the system complexity can be shared among several small central control agents, behaving like a small DMS that is able to tackle the scheduling problem of generating units (DG and microsources) and other control devices installed in the system.

It is clear that, in order to operate one or more microgrids in a coordinated way, it is important to provide a more or less decentralized decision-making process to balance demand and supply coming from both the distributed resources and the main MV distribution feeder.

2. CONTROL AND MANAGEMENT ARCHITECTURE

As previously presented, a microgrid can be defined as an LV network with several microgeneration devices (such as microturbines, PV generators, etc.) in addition to storage devices (such as flywheels, capacitor banks, etc.) and controllable loads. This system is managed in a coordinate and controlled way by a hierarchical control system that may use power cables as the physical support for a communication infrastructure. In normal operating conditions, the microgrid should operate interconnected to the main distribution network. However, the microgrid may be operated islanded from the main power system in case of contingencies in the upstream network or if maintenance actions are occurring. Therefore, the adoption and extension of the microgrid concept may enhance quality of service to final costumers, leading also to a reduction in GHG emissions and potentially reduce electric power supply costs.

The new concept of multi-microgrids is related to a high level structure, formed at the MV level, consisting of LV microgrids and DG units connected on adjacent MV feeders. This concept has been developed within the framework of European project ''More MicroGrids'' [2]. Therefore, microgrids, DG units, and MV loads under DSM control can be considered in this network as active cells, for control and management purposes. The technical operation of such a system requires the transposition of the microgrid concept to the MV level, where all these active cells should be controlled by a central autonomous management controller (CAMC) to be installed at the MV bus level of an HV/MV substation. The CAMC will serve as an interface to the DMS and operate under the responsibility of the DSO [2].

This architecture can be seen in Figure 1.

Nowadays, the DMS is responsible for the supervision, control, and management of the distribution system. In future power systems, in addition to the DMS, there will be new management levels:

1. The CAMC, to be housed in HV/MV substations, which will accommodate functionalities that are normally assigned to the DMS (or other new functionalities) and will be responsible for interfacing the DMS with lower level controllers.
2. The MicroGrid Central Controller (MGCC), to be housed in MV/LV substations, which will be responsible for managing the microgrid, including the control of the microsources and responsive

DOI: 10.1002/etep

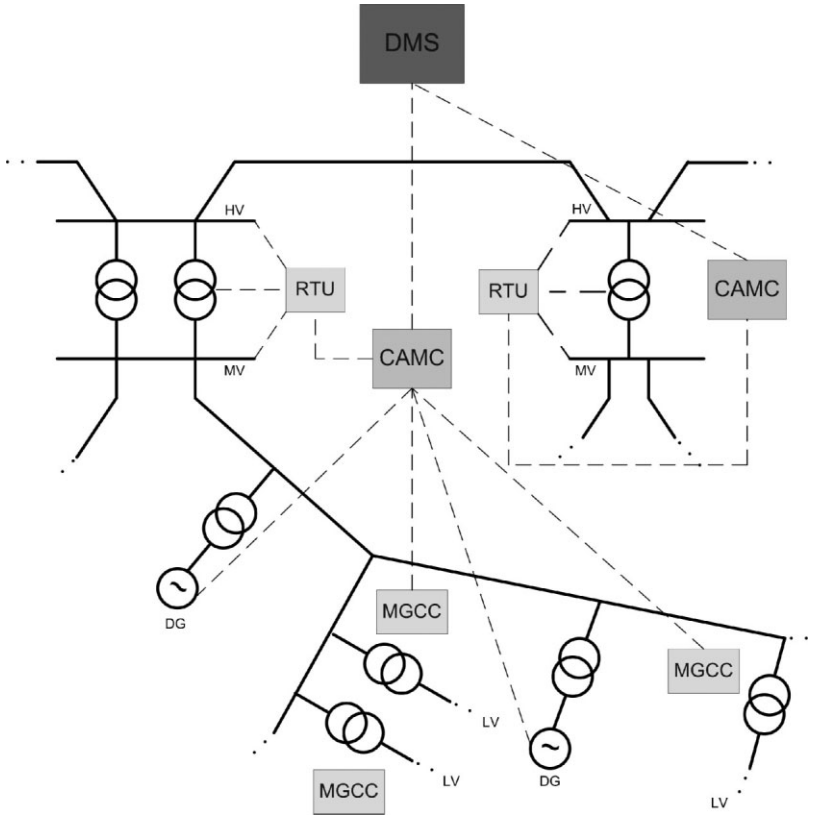

Figure 1. Control and management architecture of a multi-microgrid system.

loads. Voltage monitoring in each LV grid will be performed using the microgrid communication infrastructure.

3. CAMC FUNCTIONALITIES

Existing DMS functionalities need to be adapted due to the operational and technical changes that result from multi-microgrid operation and the introduction of the CAMC concept and corresponding hierarchical control architecture.

The management of the multi-microgrid (MV network included) will be performed through the CAMC. This controller will be responsible for acting as an intermediate to the DMS, receiving information from the upstream DMS, measurements from remote terminal units located in the MV network and existing MGCCs. It will also have to deal with constraints and contracts to manage the multi-microgrid in both HV grid-connected operating mode and emergency operating mode. A first set of functionalities to integrate the CAMC can be seen in Figure 2.

It is important to stress that not all these functionalities will be available in any multi-microgrid system. Their availability will depend on the characteristics of local DG units present.

In the next sections, two approaches to state estimation routines will be presented as well as solutions to the coordinated voltage support and frequency control problems. Three MV test networks and one LV test network have been used for testing purposes when dealing with state estimation, coordinated voltage, and frequency support.

3.1. Multi-microgrid state estimation

The multi-microgrid state estimator (MSE) follows the concepts of the distribution state estimators, receiving a limited number of real-time measurements from the multi-microgrid network [3,4]. Since

DOI: 10.1002/etep

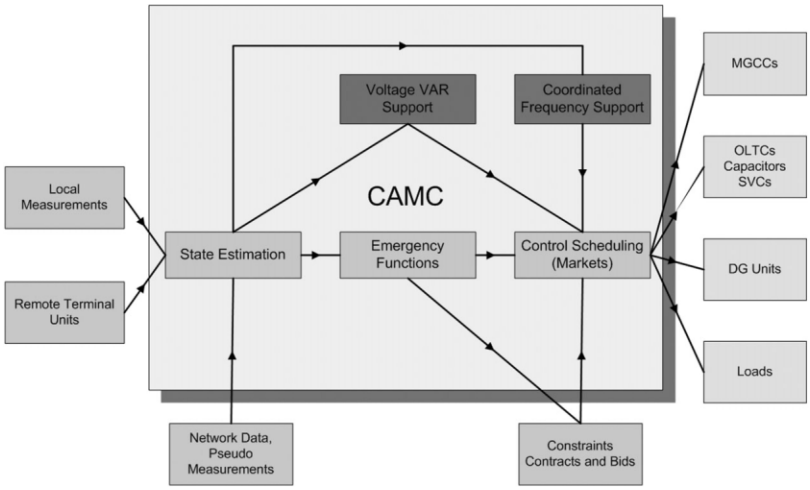

Figure 2. CAMC functionalities.

this data is inadequate for state estimation, historical or real-time load data are used to forecast node injections [5]. The measurement equations establish a relationship between *measurements* and *unknown* (*states*):

$$z = h(x) + e \tag{1}$$

Subject to:

$$c(x) = 0 \tag{2}$$

where **z** is the vector of measurements, **h**(.) is the vector of nonlinear functions relating measurements to states, **c**(**x**) is the vector function which models virtual measurements, and **e** is the measurement Gaussian error vector with $\mathbf{E}(\mathbf{e}) = 0$. The problem is formulated as an equality constrained WLS problem:

$$\min J(x) = (z - h(x))^T R^{-1}(z - h(x)) \tag{3}$$

where $R = E(ee^T) = \text{diag}(\sigma_i^2)$ is the diagonal measurement covariance matrix and σ_i is the standard deviation of the *i*th measurement. The state estimate $\hat{x}$ is obtained by solving the following system of linear equations at each iteration [6,7]:

$$F(x^k)\begin{pmatrix} \Delta x^k \\ \lambda^{k+1} \end{pmatrix} = \begin{pmatrix} H^T(x^k)R^{-1}\Delta z^k \\ \Delta c^k \end{pmatrix} \tag{4}$$

where $G(x^k) = H^T(x^k)R^{-1}H(x^k)$, $F(x^k) = \begin{pmatrix} G(x^k) & C^T(x^k) \\ C(x^k) & 0 \end{pmatrix}$, and λ are the Lagrange multipliers.

After execution of the SE algorithm the node voltage magnitudes and phase angles and (possibly) the transformer taps are estimated.

The number of customers connected to a multi-microgrid network may be large and is impractical to telemeter all points of the network. A practical MSE should have the following features:

- *Substation measurements*: The MSE must use all types of measurements available at the primary or distribution substations (feeder power flows, voltage magnitudes, current magnitudes, and circuit breaker statuses).
- *Few measurements from critical points on the network*: The network observability cannot rely on the real-time measurements. Any affordable measurements need to be critically placed on the network to reduce the standard deviation of the estimated states.

DOI: 10.1002/etep

- *Large number of customer load estimates*: The MSE must be based on a large number of forecasted load injections at each unmeasured node remote from the substations. Basically the network observability of the MSE is achieved using these measurements.
- *Distributed generators (DG)*: They are usually provided with voltage and active and reactive injection measurements which can be communicated to the principal primary substation.

The presence of large number of pseudo-load injection measurements may give rise to convergence problems. Since the accuracy of the pseudo-load injection measurements are inferior compared to the real-time measurements, improved load models are required for better convergence and voltage estimates.

In conventional state estimation the status of switching devices (switchers, breakers, fuses, sectionalizers, etc.) are processed by the network topology processor (NTP) to define the bus/branch network model, by merging bus sections joined by closed switching devices into ''nodes.'' The status of these switching devices can be telemetered or entered manually by system operators. The topology is assumed to be known and correct. The bad data processing examines only analog measurements to identify gross errors. Any status errors, that pass undetected by the NTP, result to an incorrect node/branch network model. The possibility of operating the multi-microgrid system in an isolated operating mode means that the topology of the network may not always be the same.

However, in distribution networks is not frequently possible to find and fix one topology beyond any kind of uncertainty, due to frequent changes in the topology together with the small number of existing measurement devices. In any case, it must be considered one topology to initiate the SE process but the formulation should be flexible enough to allow changes in the topology if the initial one will not lead to the best solution. This means that the topology processor must be able to consider that the identification of bad data can find errors in the status of some switching devices. This problem is solved by the generalized state estimation [8]. In generalized state estimation parts of the network are modeled at the bus-section/switching-device (physical) level. The conventional state vector is augmented with switching device statuses and other related pseudo-measurements, in order to identify topology changes and errors. This ultimately means that topology will be estimated at the same time with analog information.

An isolated island is any part of the network formed by a set of nodes connected between them and where there is no node having generation capability. The SE algorithm for an isolated island must give zero voltage magnitudes and phases in all nodes. An energized island is any part of the network formed by a set of nodes connected between them and having one or more nodes with generation capability. If this island is observable, the SE algorithm computes the island's state vector. For each island we must consider a reference node for voltage phases by fixing an arbitrary voltage phase value. However, a problem exists when the number of islands is not known when starting the SE process. This is a consequence of some switching devices having an unknown or suspicious status. In this case, the number of nodes where the voltage phase must be fixed is also unknown. The splitting problem can be formulated as the problem of finding the state variables in all network islands. This must be done even if initially the number of islands is different when compared with the result of the SE process. The consideration of uncertainty affecting topology introduces the splitting problem. Traditional SE assumes that the topology is known and fixed *a priori*. Therefore, it is assumed that the whole system consists of a unique connected island or a predefined number of islands. In this case, there is no splitting problem.

When considering uncertainties for the switching device statuses, the number of initial islands can be smaller or larger than the number of islands really existing in the system. In conventional SE formulation, splitting is impossible since there is a unique bus for phase angle reference (the whole network is one connected island). If splitting occurs, the coefficient matrix becomes singular, compromising the solution of the SE problem. When the network is split into two or more non-connected electrical islands, due to a set of switching devices reported as open, the system becomes unobservable and the state vector cannot be computed. We can implement a state estimator capable of handling multiple observable islands and reference angles, but still the correct status of those switching devices, which interconnect different islands and are erroneously reported as open, cannot be identified. In the proposed method a phase reference is used for each island, if there are more than one,

DOI: 10.1002/etep

and only one phase reference if the network is fully connected. This is done automatically by the technique shown below. Without loss of generality, we examine the $P-\delta$ state estimation problem. We consider that the multi-microgrid system is separated in r electrical (observable) islands, due to a set of switching devices being reported as open. We arbitrarily choose island 1 to contain the phase angle reference node. For each island $i \neq 1$ we provide a (critical) pseudo-measurement as follows:

$$0 = \left[\prod (1 - s_{kl})\right] \delta_{\text{ref}i} \tag{5}$$

where kl are the open switching devices whose end nodes k and l belong to islands i and $j \neq i$, respectively, and $\delta_{\text{ref}i}$ is the phase angle of the reference node of the ith island with respect to the reference node of island 1. In practice a degree of uncertainty is considered for the above pseudo-measurement, by adding a Gaussian error at the right hand side. By including $r-1$ such pseudo-measurements, the network becomes observable and the state vector can be estimated. Usually we consider two forms of topology errors:

- *Exclusion error* when a switching device actually in service is inadvertently excluded in the model.
- *Inclusion error* when a switching device is erroneously included in the state estimation model.

The proposed techniques were simulated with the test system presented in Figure 3. Data on this network can be provided on request.

The load active (MW) and reactive (Mvar) power, are based on the transformer MVA, its % loading and its load power factor:

$$\text{Load MW} = \frac{(\text{Transf.MVA}) \cdot (\text{Loading }\%) \cdot (\text{Load PF})}{100} \tag{6}$$

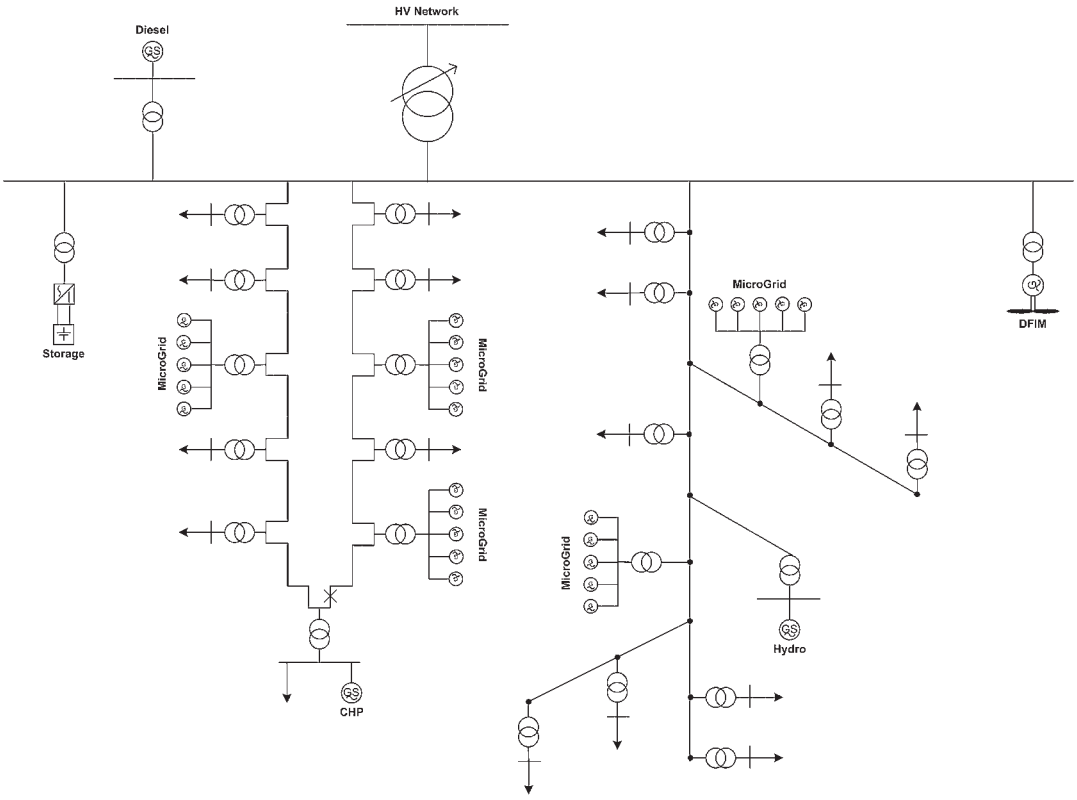

Figure 3. MV test network 1.

DOI: 10.1002/etep

$$\text{Load Mvar} = \frac{(\text{Transf.MVA}) \cdot (\text{Loading}\,\%) \cdot \sqrt{1 - (\text{Load PF})^2}}{100} \tag{7}$$

Active and reactive power generations and voltage magnitudes are measured for each DG and MV generation sites. The measurement system consists of:

- 10 voltage magnitude measurements at generation nodes (*real-time*), including the reference node;
- 7 pairs of active and reactive flow measurements (*real-time*), at all lines and transformers around MV node;
- 10 pairs of active and reactive generation injection measurements (*real-time*);
- 16 pairs of active and reactive loads (*pseudo*) at LV nodes;
- 29 active and 27 reactive zero injections (*perfect*);
- 2 reactive injection measurements (*real-time*) at capacitor banks.

The measurement redundancy is low and the error filtering capability of the state estimator is very low. We considered that the network is in grid-connected mode (one connected area). A single bad data at a load of feeder 1 is examined. The true and the measured data are $0.838\,\text{MW} + 0.275\,\text{Mvar}$ and $1.2\,\text{MW} + 0.35\,\text{Mvar}$, respectively. The faulty load value affected mainly the nodes of feeder 1 and the reference node (Figures 4 and 5). The normalized residuals of the active and reactive injection (load) measurements were $|-4.78| > 3$ and $|-3.78| > 3$, respectively, indicating gross error. After removing these measurements and re-computing the state vector all the normalized residuals became <3.

From the state estimation runs it is shown that error in a load value affects mainly the node voltages of the feeder where this load belongs. The primary MV substation acts as a burden to the error spread to other feeders. Voltage phase angles are more sensitive to errors than voltage magnitudes. When applied to real multi-microgrids, the solution algorithm convergence and the state estimate accuracy mostly depend on the accuracy of the load models. Validation with actual measured data is the key for improving the load models.

3.2. Fuzzy state estimation

The state estimation problem is solved by using all the information available for the network, not only measurement values. Of course, the quality of the solution turns better as the quality of the available

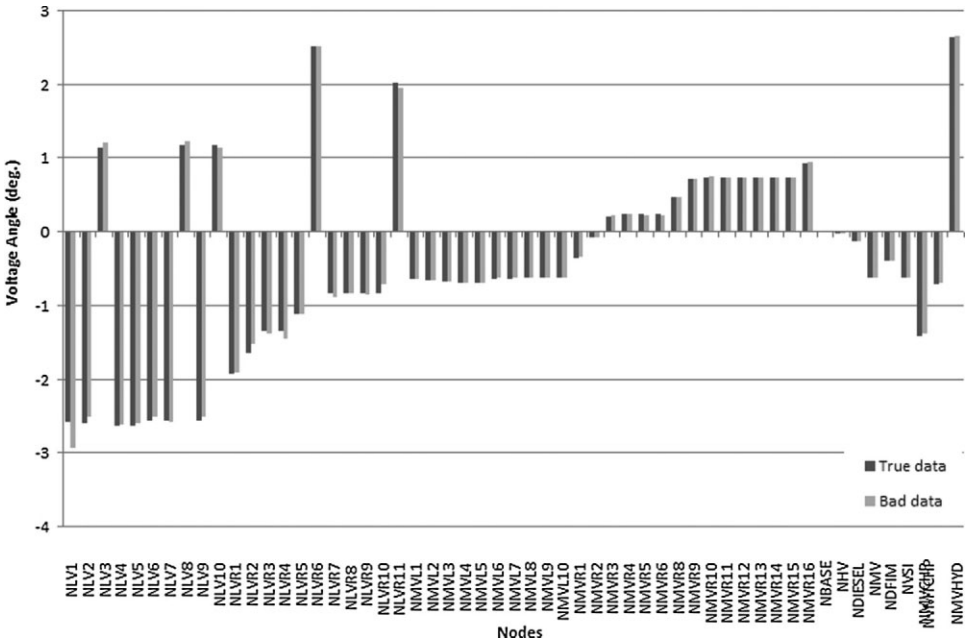

Figure 4. True and estimated node voltage phase angles.

DOI: 10.1002/etep

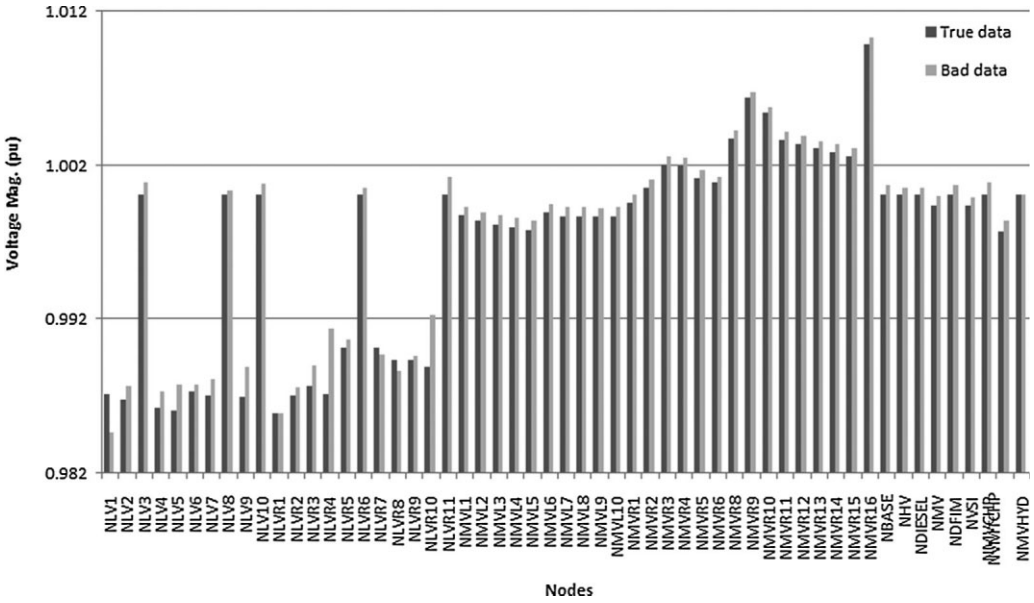

Figure 5. True and estimated node voltage magnitudes.

information improves. In the fuzzy state estimation (FSE) model [9], we can use also information affected by uncertainty by using fuzzy sets theory [10]. We use fuzzy numbers to model this kind of information and we call fuzzy measurements to these numbers used as input data for the model.

One source of fuzzy measurements is obtained from some ''typical'' load curve that defines a band of possible values for the power consumption, based possibly on past history saved in a historical database. Using this, it is possible to define a fuzzy assessment for the actual active load value.

If the microgrid generation is not measured, a procedure to define a fuzzy measurement can be used based on the mix of type of technology and all useful forecasted values available. The same is valid for DG connected directly to the MV grid, if it is not measured.

Another way to obtain fuzzy measurements corresponds to the use of a fuzzy load allocation algorithm [11]. This algorithm consists of an allocation process of load values admitting some ranges of uncertainty. By this algorithm, we perform a first allocation process using the available information. After this, we correct these values using the FSE process. The first set of values is represented using intervals corresponding to ranges of uncertainty and having the greatest possibility degree.

An alternative process to obtain uncertain information corresponds to translate natural language propositions obtained from experienced operators since they typically have lots of qualitative information expressed in a non-mathematical way.

The mathematical formulation of the FSE process can be described by a vectorial expression (8) using the following notation: $\mathbf{Z}$ represents the measurement vector (which includes fuzzy measurements); $\mathbf{X}$ represents the fuzzy state vector; $\mathbf{h}(.)$ represents the function vector that relates the state variables and the measurements; and ε represents the fuzzy noise vector between the measurement value and the evaluated value using the corresponding power flow function:

$$\mathbf{Z} = \mathbf{h}(\mathbf{X}) + \varepsilon \tag{8}$$

In the first phase of the FSE algorithm, the crisp measurement vector, resulting from the measurements decomposition, will be used to run a crisp WLS state estimation algorithm to compute the state vector $\mathbf{X}_C$. In the second phase of the FSE algorithm, the fuzzy deviations specified for the measurements are reflected on the results of the state estimation. These results are obtained using the state vector $\mathbf{X}_C$, the gain matrix inverse $\mathbf{G}^{-1}$, and the Jacobian matrix $\mathbf{H}$ computed in the last iteration of the first phase of this algorithm applying expression using (9). With this expression the fuzzy state

DOI: 10.1002/etep

vector **X** is obtained:

$$\mathbf{X} = \mathbf{X_C} + \left[\mathbf{G^{-1}H^T R^{-1}}\right] \times [\mathbf{Z} - \mathbf{h}(\mathbf{X_C})] \tag{9}$$

Also active and reactive power flows, currents in lines and transformers, power injected by generators or by connections with other networks, active and reactive load values are computed using these matrixes and similar operations [9].

The studies conducted to evaluate the effectiveness of the FSE were performed on the test system shown in Figure 3.

This intends to simulate the following conditions: all communications with microgrids are missing; all communications with DG are missing. It was used qualitative data for these missing measures, represented by fuzzy measurements (an example in Figure 6).

The FSE algorithm is executed under the above-defined conditions to produce an estimation of bus voltages (both module and phase) (Figure 7). Other results obtained from the state estimation algorithm are the values for the power injections for each bus (Figure 8), power flows, and current on each branch (Figure 9).

A comment related with these membership functions is that the central values of the initially specified and computed membership functions for the active and reactive power injection are slightly shifted. This is understandable considering that this set of values is used to perform the initial crisp state estimation study aiming at obtaining a coherent operating point of the system. This means that,

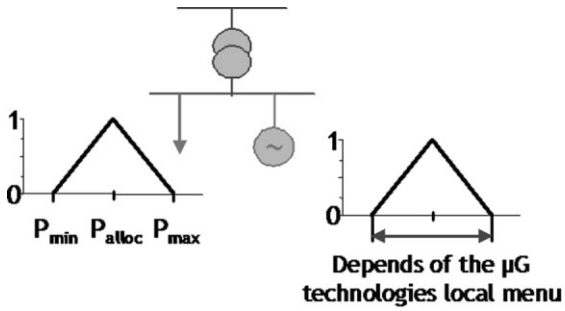

Figure 6. Type of fuzzy information considered on the microgrids.

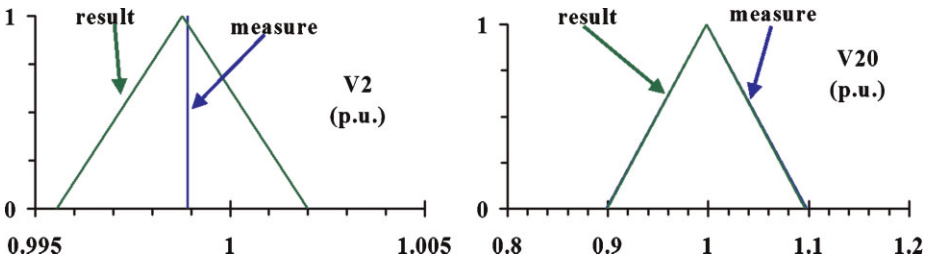

Figure 7. Membership functions for the measurements and for the results of the voltage magnitude in the buses 2 and 20.

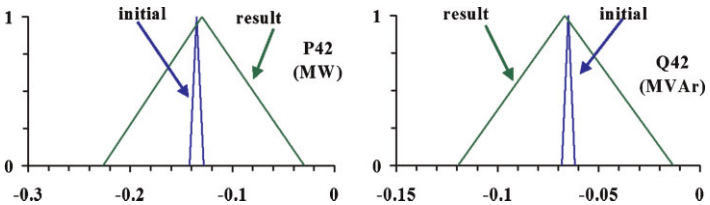

Figure 8. Membership functions for the measurements and for the results of the active and reactive power injected on bus 42.

DOI: 10.1002/etep

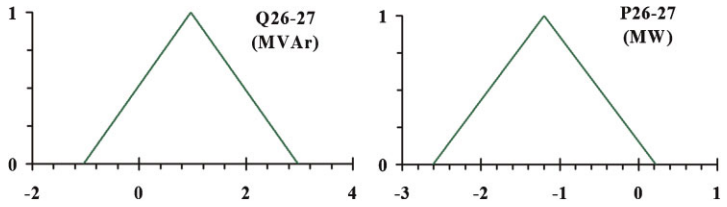

Figure 9. Membership functions for the measurements and for the results of the active and reactive power flow on the branch connecting buses 26 and 27.

due to metering errors and to fuzzy assessments, this set of input values does not correspond to a coherent picture possibly not being in accordance with Kirchoff laws.

For instance, the result for the reactive power flow in Figure 9 can have the following interpretation: the value of the reactive power flow is 1.2 Mvar with 1.0 membership degree, but has a possibility of having a value between -0.2 and 2.6 Mvar.

3.3. Coordinated voltage support

A novel methodology for coordinated voltage support for multi-microgrid systems was developed based on the work presented in [12]. This functionality aims at optimizing distribution network operation in interconnected mode, when dealing simultaneously with DG connected directly to the MV grid and microgeneration installed at the LV side.

Considering that in LV networks the line resistance can be greater than the line reactance (i.e., $R \gg X$), traditional control strategies using only reactive power control may not be sufficient in order to perform efficient voltage control since active/reactive power decoupling is not valid [13]. This can be seen from (10), derived from the power flow equations in a line, according to Figure 10.

$$P_{12} = \frac{V_1^2 - V_1 V_2 \cos(\theta_{12})}{R} \tag{10}$$

In addition, in scenarios with high microgeneration penetration, generation shedding actions may also be needed in order to limit the voltage rise effect resulting from massive microgeneration penetration. The control algorithm proposed uses all traditional control approaches for voltage and reactive power control namely managing on-load tap changing (OLTC) transformers, reactive power provided by DG sources, and capacitor banks together with active power control at the microgrid level in extreme scenarios (using microgeneration shedding mechanisms).

The coordinated voltage control problem is a nonlinear optimization problem containing both continuous and discrete variables that can be formulated as presented in (11) and (12):

$$\min \sum \mu G_{\text{shed}} \tag{11}$$

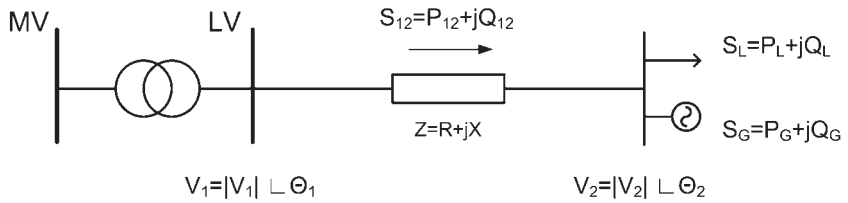

Figure 10. Power flow in a line.

DOI: 10.1002/etep

Subject to:

$$\begin{aligned}
&P_i^G - P_i^L = \sum_{k=1}^{N} V_i V_k (G_{ik}\cos(\theta_{ik}) + B_{ik}\sin(\theta_{ik})) \\
&Q_i^G - Q_i^L = \sum_{k=1}^{N} V_i V_k (G_{ik}\sin(\theta_{ik}) - B_{ik}\cos(\theta_{ik})) \\
&V_i^{\min} \le V_i \le V_i^{\max} \\
&S_{ik}^{\min} \le S_{ik} \le S_{ik}^{\max} \\
&t_i^{\min} \le t_i \le t_i^{\max} \\
&Q_i^{\min} \le Q_i \le Q_i^{\max}
\end{aligned} \tag{12}$$

where μG_{shed} is the amount of microgeneration shed; P_i^G, P_i^L the active power generation/consumption at bus i; V_i the voltage at bus i; G_{ik} the real part of the element in the admittance matrix (*Ybus*) corresponding to the ith row and kth column; B_{ik} the imaginary part of the element in the *Ybus* corresponding to the ith row and kth column; θ_{ik} the difference in voltage angle between the ith and kth buses; Q_i^G, Q_i^L the reactive power generation/consumption at bus i; $V_i^{\min}$, $V_i^{\max}$ the minimum and maximum voltage at bus i; S_{ik} the power flow in branch ik; $S_{ik}^{\min}$, $S_{ik}^{\max}$ the minimum and maximum power flows in branch ik; t_i the transformer tap of or capacitor step position; and $t_i^{\min}$, $t_i^{\max}$ the minimum and maximum tap.

An optimization tool based on a meta-heuristic approach (evolutionary particle swarm optimization) was developed to address the coordinated voltage control problem at MV and LV levels [14,15]. It uses an artificial neural network (ANN) to emulate the behavior of the LV microgrid system.

The voltage control scheme approach developed was intended to be used as an online function, made available to the DSO. Nevertheless, in order to be able to have a simulation tool that can effective and efficiently optimize in a coordinated way the MV and LV networks, some adaptations to the methodology used in the control algorithm must be made.

Firstly, regarding the coordinated operation at the MV and LV levels, a combined and uniform approach must be followed. In order to address this issue, an ANN able to emulate the behavior of the LV network (or microgrid) was developed. This option enables the use of a traditional power flow routine for the MV, ensuring a decoupling of the two voltage levels, without compromising the validity and quality of the results and three-phase power flow module for the LV side.

Secondly, the use of an ANN is able to speed up the algorithm, thus enabling the use of the meta-heuristic tool employed in real-time operation, reducing the long simulation times that were required in order to calculate consecutive three-phase power flows.

The ANN used is presented in Figure 11.where V_{sp} is the voltage at the MV/LV substation; $\Sigma P\text{g}_{\text{p}i}$ the total active power generation in phase i; $\Sigma P\text{l}_{\text{p}i}$ the total active power load in phase i; $P\text{loss}_{\text{p}i}$ the total active power losses in phase i; and $V\text{max}_{\text{p}i}$ the maximum voltage value in phase i.

Some of the main results obtained using MV and LV test networks are presented next. The networks used are based on real typical Portuguese rural grids and have a radial structure. The MV network contains several DG units (mostly based on hydro and wind generation) and microgrids and is shown in

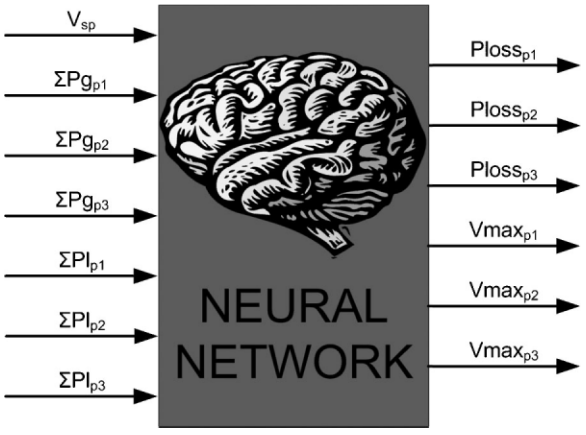

Figure 11. Artificial neural network for microgrid emulation.

DOI: 10.1002/etep

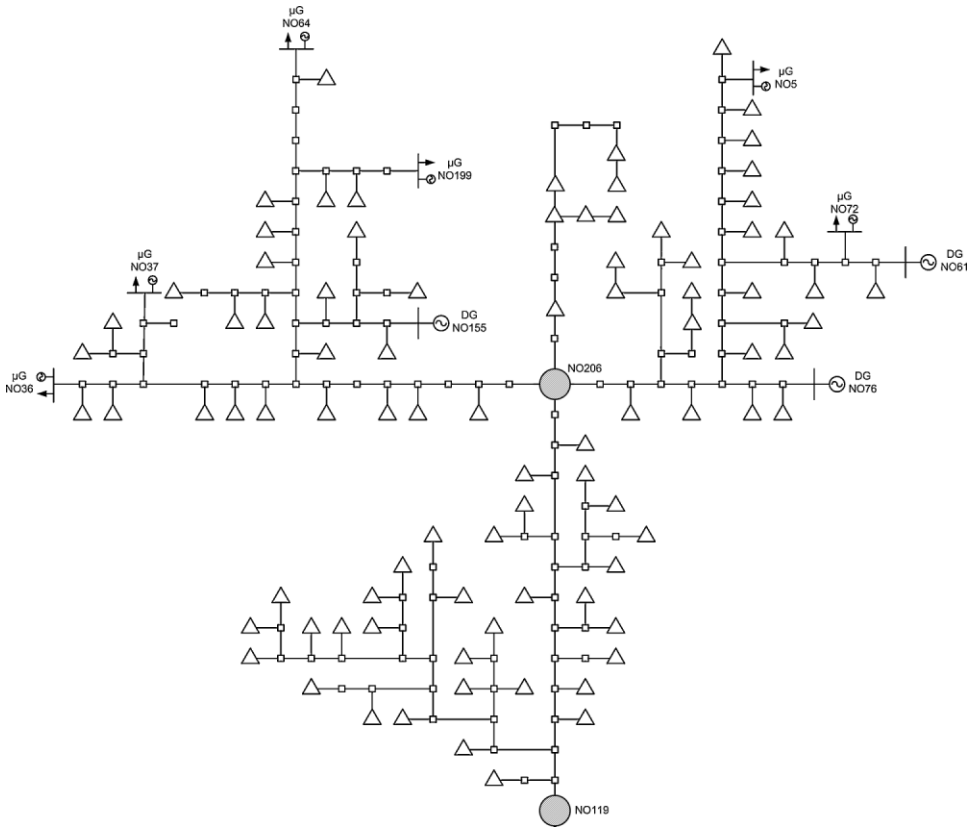

Figure 12. MV test network 2.

Figure 12. The LV microgrid is assumed to contain a massive penetration of PV-based generation and is presented in Figure 13. Data on these networks can be provided on request.

Figure 14 compares the base situation without the voltage control functionality (Initial) and the result obtained from the application of the control algorithm (Final) in the LV microgrid for each of the 24 hours of a typical day. It can be seen that the voltage values were out of an admissible range of $\pm 5\%$ due to the massive penetration of PV-based microgeneration that generated power outside the peak demand hours but the algorithm succeeded in bringing voltage profiles back to admissible values.

Figure 15 shows that some microgeneration shedding was required (difference between Initial and Final values for microgeneration) in order to bring voltage profiles back within admissible limits (presented in Figure 14).

3.4. Coordinated frequency control

A methodology for coordinated frequency control for multi-microgrid systems was also developed. The main objective is to allow a robust islanded operation and also to support the islanding transition. In order to accomplish this, the CAMC includes an additional functionality of coordinated frequency support that reacts to power system frequency changes in a way similar to the one implemented in regular automatic generation control (AGC) functionalities [16].

The frequency of the system is continuously monitored by the CAMC (Figure 16). At every time interval T_s (sample time), if triggered by significant changes in frequency, the CAMC will send control set-points to every MGCC, other DG units, and controllable loads [17]. This sample time T_s cannot be very small, mainly because of the constraints imposed by the communication system.

Therefore, the frequency error and the frequency error integral will be used to determine the additional power ΔP – as presented in (13) – to be requested to the available contributors under CAMC

DOI: 10.1002/etep

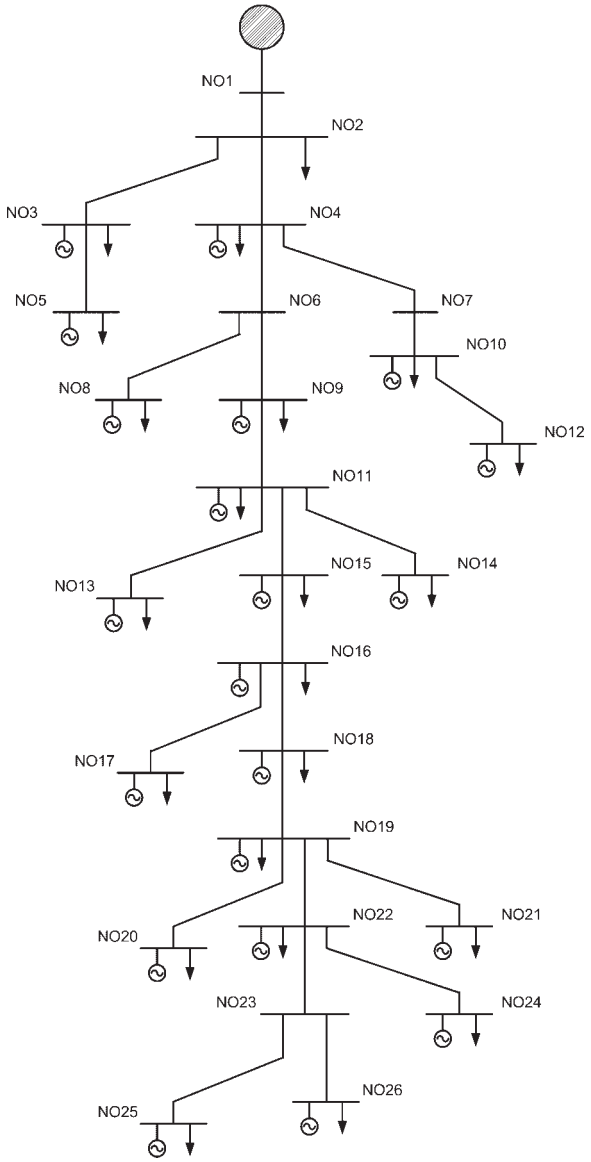

Figure 13. LV test network (microgrid).

control: MGCCs, DG units, and controllable MV loads.

$$\Delta P = \left(K_{\mathrm{P}} + K_{\mathrm{I}} \frac{1}{s}\right) \times (f_{\mathrm{rated}} - f) \tag{13}$$

where K_{P} is the predefined proportional gain; K_{I} the predefined integral gain; f_{rated} the nominal frequency value; and f the actual frequency value.

It should be noted that this additional power may be negative if the frequency rises over the rated value. In this way the CAMC can also respond to other disturbances, such as load loss while in islanded mode, managing generation sources to reduce their power output (including microgeneration curtailment, if necessary).

However, limits have to be enforced on the value of ΔP. Its value cannot be larger than the available reserve and, if ΔP is negative, its absolute value cannot be lower than the total generation available for curtailment.

DOI: 10.1002/etep

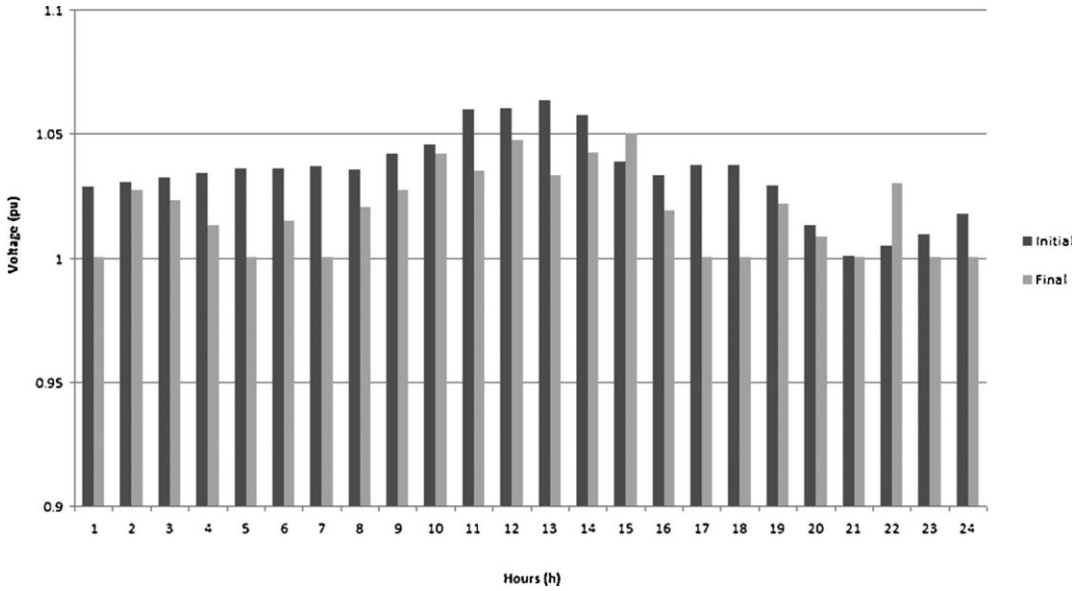

Figure 14. Maximum voltage values inside a microgrid.

If the absolute value of the required power variation ΔP is larger than a predefined threshold (related to a dead-band), the control system will proceed to determine how to optimally distribute the power requests among the available sources. Unitary generation costs for each of the sources (MGCCs and other DG) are used for this purpose. The economical allocation algorithm is based on standard linear optimization techniques:

$$\begin{aligned} & \min_x z = c^T x \\ \text{subject to} \quad & \sum x = \Delta P \\ & x \geq b_1 \\ & x \leq b_2 \end{aligned} \tag{14}$$

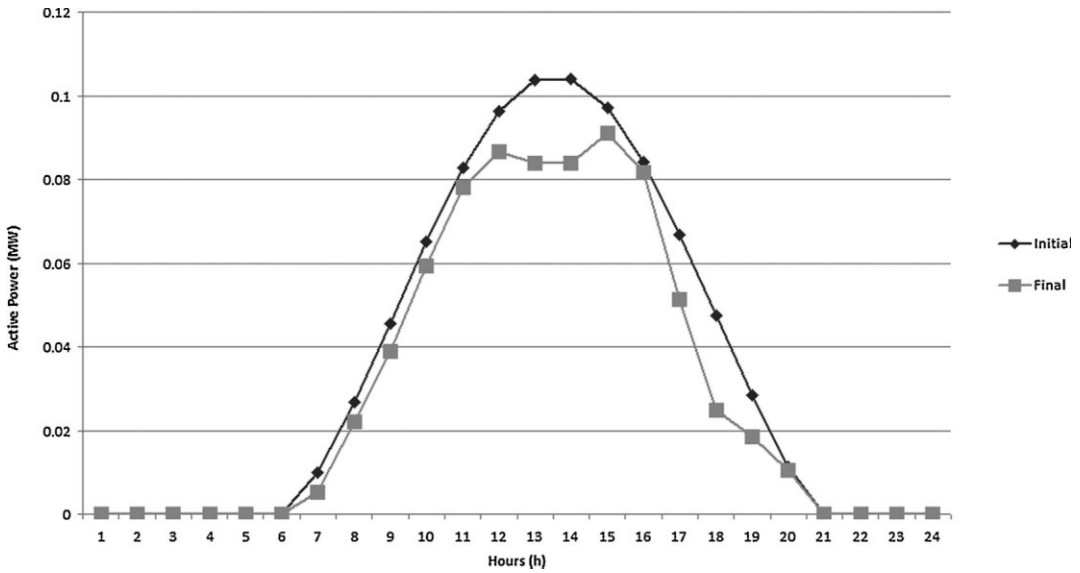

Figure 15. Total microgeneration inside a microgrid.

DOI: 10.1002/etep

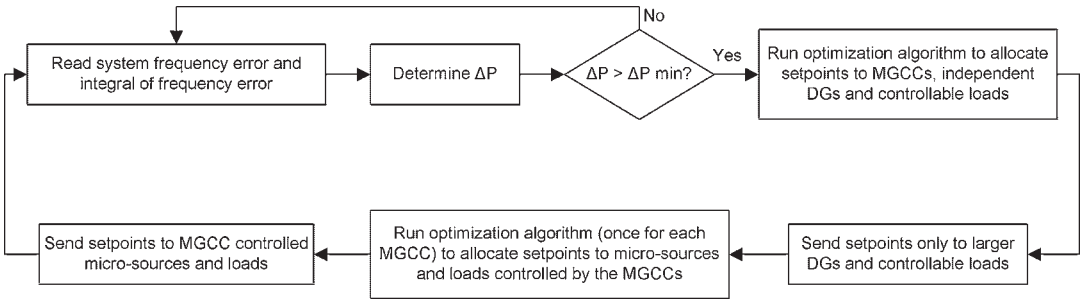

Figure 16. Implementation flowchart.

where c is the generation cost and load curtailment prices; x the generation or load set-point variations; b_1 the smallest variations allowed (lower bounds); and b_2 the largest variations allowed (upper bounds).

The set of above restrictions can also define which generators/loads participate in frequency regulation. This can be done by setting to zero the ith elements of both b_1 and b_2 corresponding to units that cannot be adjusted.

Because loads are considered as negative generation, the corresponding coefficients (elements in vector **c** of prices) are negative.

This optimization procedure is performed for each period T_s and will originate a vector representing the power generation changes to be requested to microgrids (MGCCs), independent DG units (e.g., CHP) and loads (MV load-shedding operations).

Each MGCC will now use the power change requested by the CAMC to establish the main restriction of a new optimization procedure (identical to the one used before by the CAMC) which will determine the power changes to be requested to microsources and controllable loads under MGCC control. Some of these microsources do not have regulation capabilities (e.g., PV or wind generation, due to limitations in primary resource availability) and will not normally be asked to change power generation.

It should be noted that the approach to load shedding is, in this context, fairly different from the one used in conventional systems, as the controllable loads will be under hierarchical control system supervision which is not capable of acting in near instantaneous time frames, mainly due to communication system limitations. Therefore, in these circumstances, load shedding is not expected to reduce the amplitude of frequency excursions in the few seconds following a severe disturbance. This load shedding capability should be seen more as a kind of secondary reserve – rather than an emergency resource – aiding the frequency to return to the rated value faster or without depending so much on the availability of renewable resources or other generation systems.

The adopted test network represents what could possibly be the typical structure of an MV grid containing multiple microgrids and several kinds of larger DG systems (Figure 17).

This network has four zones: two rural areas and two urban areas (the loops on the left of Figure 17), connected to an HV/MV substation. There is also a relatively large number of microgrids, all connected to MV buses, and also some other typically DG-oriented-generation systems: a small diesel group, several CHP and hydro units, two doubly-fed induction machines (DFIM) corresponding to wind-generator systems, and a storage element interfaced with the MV grid via a voltage source inverter (VSI).

All microgrids have a 150 kW/50 kvar equivalent controllable load and also the same mix of microsources: a small wind generator, a fuel cell, a microturbine, a photovoltaic generator, and a storage element connected to the grid via a VSI (representing storage elements).

The test case analyzed shows a situation where the MV network containing the microgrids is importing approximately 5.3 MW of active power from the upstream HV network, in order to be able to supply a total load of 19.9 MW. Starting from this point, in steady state, the HV/MV branch is disconnected at $t = 10$ seconds and the multi-microgrid system will become islanded. In order to evaluate the load following capabilities of this control approach, it was assumed that at $t = 110$ seconds the load at several nodes begins to change at a rate of 4% per second for 10 seconds (for total increase of nearly 0.9 MW).

DOI: 10.1002/etep

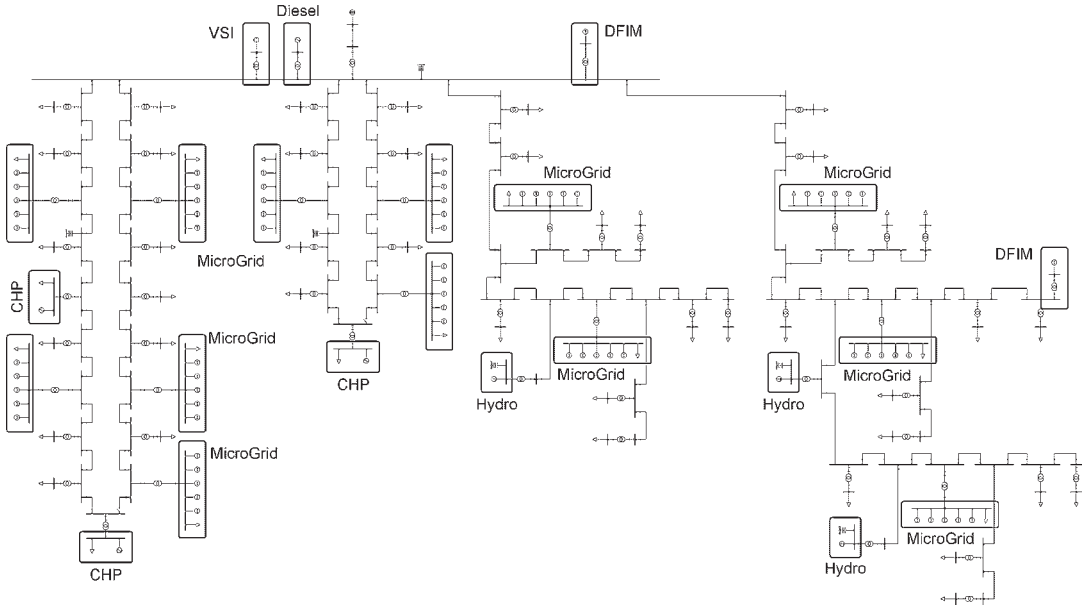

Figure 17. MV test network 3.

For this case the sample time in use is $T_s = 5$ seconds. Lower values can accelerate the response of the system but, even if technically possible to attain, they could also originate some stress on the control system. The most adequate value will ultimately depend on the communication system in use and on the mix of microsources and other DG units on the system.

Figure 18 shows how the hierarchical control present in this multi-microgrid manages to recover the frequency to the rated value after the islanding occurred. Although the minimum frequency value after the disturbance remains practically unaltered, the presence of the hierarchical control assures that the system is capable to return to its nominal frequency.

The frequency recovery is due to the fact that the CAMC is sending set-points to the microgrids and other DG units in the MV network. In Figure 19, the set-points sent to one of the microgrids and to one of the CHP units are shown, together with the corresponding output power. The order by which the microgrids or the DG units start to contribute is based on their cost as a direct consequence of the

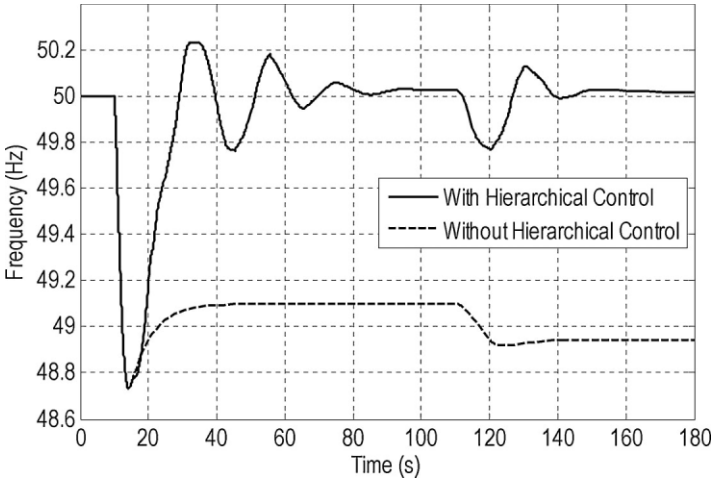

Figure 18. Frequency with and without hierarchical control.

DOI: 10.1002/etep

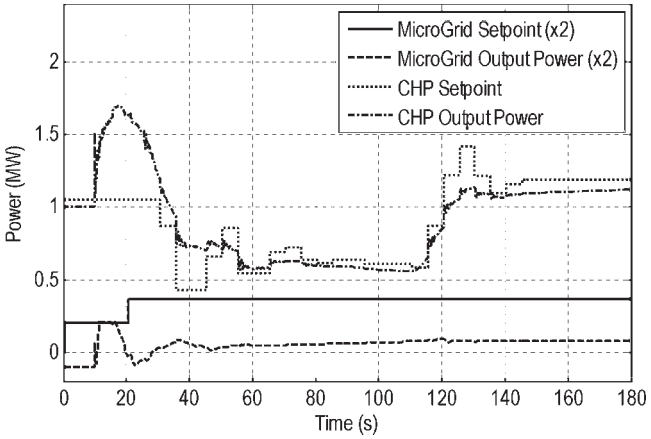

Figure 19. Example of set-point commands and output powers.

optimization method adopted. Therefore, in this case, it becomes clear that the microgrids are considered to be less expensive than the CHP unit.

Figure 19 also shows how the algorithm is ready to shed generation in case the frequency rises above the rated value (generation curtailment).

4. CONCLUSIONS

The definition of an effective control scheme for multi-microgrid operation is a key issue. In particular, it is extremely important the introduction of a new main controller – the CAMC – that includes several key functionalities such as coordinated voltage support, coordinated frequency support, and local state estimation. The control strategy for multi-microgrid operation proposed in this paper is based on a hierarchical and decentralized scheme, ensuring both autonomy and redundancy.

The multi-microgrid state estimation is based on a limited number of real-time measurements and forecasted node injections. The proposed algorithm was very robust and load injection errors were limited in the load neighborhood. As a consequence it can be efficiently used for local state estimation.

An FSE methodology aiming at identifying the state of distribution networks with large number of microgrids was developed. This model is highly flexible in terms of the data it can incorporate. It can include traditional real-time measurements, fuzzy evaluations, and results from load allocation procedures. This means that an enlargement of the traditional probabilistic nature of WLS state estimation algorithms to deal with data having uncertainty using fuzzy concepts. This reflects a desire to use the most adequate mathematical tools for each particular situation.

The optimization algorithm developed in order to deal with the coordinated voltage support has proved to be efficient in maintaining voltage profiles within admissible limits in a scenario with high microgeneration penetration.

Tasks related to coordinated frequency control were successfully fulfilled, either after islanding or for load-following purposes. The set-point modification commands sent to the DG units, microgrids, and controllable loads, enable the frequency to return to the rated value in a reasonable amount of time.

5. LIST OF SYMBOLS AND ABBREVIATIONS

5.1. Symbols

z	is the vector of measurements
$h(.)$	is the vector of non-linear functions relating measurements to states
$c(x)$	is the vector function which models virtual measurements
e	is the measurement Gaussian error vector with $E(e) = 0$
$R = E(ee^T) = diag(\sigma_i^2)$	is the diagonal measurement covariance matrix

DOI: 10.1002/etep

$\hat{x}$	is the state estimate
σ_i	is the standard deviation of the *ith* measurement
λ	are the Lagrange multipliers.
$k-l$	are the open switching devices whose end nodes k and l belong to islands i and $j \neq i$ respectively
δ_{refi}	is the phase angle of the reference node of the *ith* island with respect to the reference node of island 1
Z	is the measurement vector (which includes fuzzy measurements)
X	is the fuzzy state vector
ε	is the fuzzy noise vector between the measurement value and the evaluated value using the corresponding power flow function
X_C	is the state vector
G^{-1}	is the gain matrix inverse
H	is the Jacobian matrix computed in the last iteration of the first phase of this algorithm
X	is the fuzzy state vector
μG_{shed}	is the amount of microgeneration shed
P_i^G, P_i^L	are the active power generation/consumption at bus i
V_i	is the voltage at bus i
G_{ik}	is the real part of the element in the Admittance Matrix (*Ybus*) corresponding to the i^{th} row and k^{th} column
B_{ik}	is the imaginary part of the element in the *Ybus* corresponding to the i^{th} row and k^{th} column
θ_{ik}	is the difference in voltage angle between the i^{th} and k^{th} buses
Q_i^G, Q_i^L	is the reactive power generation/consumption at bus i
V_i^{min}, V_i^{max}	ate the minimum and maximum voltage at bus i
S_{ik}	is the Power flow in branch ik
S_{ik}^{min}, S_{ik}^{max}	are the minimum and maximum power flows in branch ik
t_i	is the transformer tap of or capacitor step position
t_i^{min}, t_i^{max}	are the minimum and maximum tap
V_{sp}	is the voltage at the MV/LV substation
ΣPg_{pi}	is the total active power generation in phase i
ΣPl_{pi}	is the total active power load in phase i
$Ploss_{pi}$	is the total active power losses in phase i
$Vmax_{pi}$	is the maximum voltage value in phase i
K_P	is the predefined proportional gain
K_I	is the predefined integral gain
f_{rated}	is the nominal frequency value
f	is the actual frequency value
c	is the generation cost and load curtailment prices
x	is the generation or load set-point variations
b_1	is the smallest variations allowed (lower bounds)
b_2	is the largest variations allowed (upper bounds)

5.2. Abbreviations

AGC	Automatic Generation Control
ANN	Artificial Neural Network
CAMC	Central Autonomous Management Controller
CHP	Combined Heat and Power
DG	Distributed Generation
DMS	Distribution Management System
DSM	Demand Side Management
DSO	Distribution System Operator

DOI: 10.1002/etep

FSE	Fuzzy State Estimation
GHG	Green House Gases
HV	High Voltage
LV	Low Voltage
MGCC	MicroGrid Central Controller
MSE	Microgrid State Estimator
MV	Medium Voltage
NTP	Network Topology Processor
OLTC	On-Line Tap Changing
RTU	Remote Terminal Unit
SE	State Estimation
WLS	Weighted Least Squares

ACKNOWLEDGEMENTS

This work was supported in part by the European Commission within the framework of the More MicroGrids project, Contract No. 019864 (SES6). The authors would like to thank the research team of the More MicroGrids project for valuable discussions and feedback. A. G. Madureira wants to express his gratitude to Fundação para a Ciência e a Tecnologia (FCT), Portugal, for supporting this work under the grant SFRH/BD/29459/2006. N. J. Gil also wants to express his gratitude to Fundação para a Ciência e a Tecnologia (FCT), Portugal, for supporting this work under the grant SFRH/BD/38194/2007.

REFERENCES

1. Peças Lopes JA, Moreira CL, Madureira AG. Defining control strategies for microgrids islanded operation. *IEEE Transactions on Power Systems* 2006; **21**(2):916–924.
2. European Research Project. ''Advanced Architectures and Control Concepts for MORE MICROGRIDS'' [Online] http://www.microgrids.eu/index.php, accessed May 2009.
3. Thornley V, Jenkins N, White S. ''State estimation applied to active distribution networks with minimal measurements'', *15th Power Systems Computation Conference*, Liege, Belgium, August 2005.
4. Cobelo I, Shafiu A, Jenkins N, Strbac G. State estimation of networks with distributed generation. *European Transactions on Electrical Power* 2006; **17**(1):21–36.
5. Ghosh AK, Lubkeman DL, Jones RH. Load modeling for distribution circuit state estimation. *IEEE Transactions on Power Delivery* 1997; **12**(2):999–1005.
6. Aschmoneit FC, Peterson NM, Adrian EC. ''State estimation with equality constraints'', *Power Industry Computer Applications Conference*, Toronto, May 1977; 427–430.
7. Korres GN. A robust method for equality constrained state estimation. *IEEE Transactions on Power Systems* 2002; **17**(2):305–314.
8. Monticelli A. State estimation in electric power systems: a generalized approach. *Kluwer's Power Electronics and Power Systems Series*. Norwell, 1999; 267–282.
9. Pereira J. ''A state estimation approach for distribution networks considering uncertainties and switching'', PhD Thesis, Faculdade de Engenharia da Universidade do Porto, Porto, July 2001. [Online] http://saca.inescporto.pt/artigos/artigo150.pdf, accessed May 2009.
10. Zadeh LA. Fuzzy sets. *Information and Control* 1965; **8**:338–353.
11. Miranda V, Pereira J, Saraiva JT. Load allocation in DMS with a fuzzy state estimator. *IEEE Transactions on Power Systems* 2000; **15**(2):529–534.
12. Madureira AG, Peças Lopes JA. ''Voltage and reactive power control in MV networks integrating microgrids'', *International Conference on Renewable Energy and Power Quality*, Seville, Spain, March 2007. [Online] http://www.icrepq.com/icrepq07/386-madureira.pdf, accessed May 2009.
13. Jenkins N, Allan R, Crossley P, Kirschen D, Strbac G. Embedded generation. *IET Power and Energy Series*. London, 2000; **31**:11–13.
14. Peças Lopes JA, Madureira AG. ''A voltage control optimization for distribution networks with DG and micro-Grids'', *Optimization Advances in Electric Power Systems*, Nova Publishers, Chapter 5, 87–112, December 2008.
15. Madureira AG, Peças Lopes JA. Coordinated voltage support in distribution networks with distributed generation and microgrids. *IET Renewable Power Generation* 2009; **3**(4):439–454.
16. Kundur P. *Power System Stability and Control*. McGraw-Hill: New York, 1994.
17. Gil NJ, Peças Lopes JA. Hierarchical frequency control scheme for islanded multi-microgrids operation. *IEEE PES PowerTech '07*, Lausanne, Switzerland, July 2007.